Available online at www.sciencedirect.com
SCIENCE DIRECT®
Journal of Power Sources 126 (2004) 169–174
JOURNAL OF POWER SOURCES
www.elsevier.com/locate/jpowsour

Influence of microstructure on the electrochemical performance of $LiMn_{2-y-z}Li_yNi_zO_4$ spinel cathodes in rechargeable lithium batteries

Youngjoon Shin, A. Manthiram*

Materials Science and Engineering Program, The University of Texas at Austin, Austin, TX 78712, USA

Received 4 June 2003; accepted 8 September 2003

Abstract

$LiMn_{2-y-z}Li_yNi_zO_4$ ($0 \le y \le 0.075$ and $0 \le z \le 0.075$) cathodes have been synthesized by two procedures at 800 °C in air: (1) standard solid state reactions of Li_2CO_3, Mn_2O_3 and NiO (oxide method) and (2) reaction of a $Li_{\sim 0.5}MnO_2$ precursor supplied by a commercial firm with lithium and nickel hydroxides (precursor method). The samples have been characterized by X-ray diffraction, surface area, manganese dissolution, scanning electron microscopy, and electrochemical charge–discharge measurements. The co-substituted $LiMn_{2-y-z}Li_yNi_zO_4$ ($0.04 \le y \le 0.075$ and $0.05 \le z \le 0.075$) samples obtained by both the oxide and precursor methods exhibit superior capacity retention, rate capability, and storage characteristics compared to both $LiMn_2O_4$ and $LiMn_{1.97}Li_{0.03}O_4$. While the rate capability and storage characteristics of the $LiMn_{2-y-z}Li_yNi_zO_4$ samples do not differ significantly between the two synthesis procedures, the samples obtained by the precursor method exhibit slightly better capacity retention despite a higher amount of manganese dissolution than the samples obtained by the oxide method. The differences are attributed to the larger and more uniform size of the secondary particles and smaller primary particles of the former compared to those of the latter.
© 2003 Elsevier B.V. All rights reserved.

PACS: 84.60.Dn

Keywords: Lithium-ion battery; Spinel manganese oxide; Electrochemical properties

1. Introduction

Lithium-ion batteries have become attractive power sources for portable electronic devices such as cellular phones and laptop computers. However, the high cost and toxicity associated with the currently used $LiCoO_2$ cathodes are forcing the development of alternative less expensive cathodes particularly for applications such as electric vehicle. In this regard, the spinel $LiMn_2O_4$ has become appealing since Mn is inexpensive and environmentally benign. However, the $LiMn_2O_4$ cathodes are plagued by severe capacity fade particularly at elevated temperatures. Several mechanisms such as Jahn Teller distortion [1], manganese dissolution [2–4], loss of crystallinity [5,6], formation of two cubic phases [7,8], and development of microstrain [9] during cycling have been proposed to account for the capacity fade. Different strategies have been pursued over the years to overcome capacity fade of $LiMn_2O_4$ [4–16], and the substitutions of other cations M^{n+} for manganese to give $LiMn_{2-y}M_yO_4$ (M = Li, Cr, Fe, Co, Ni, and Cu) have been found to improve the cyclability.

We showed recently that a co-substitution of small amounts of both Li and Ni for Mn to give $LiMn_{2-2y}Li_yNi_yO_4$ ($0.05 \le y \le 0.1$) is more effective in improving the electrochemical properties than single substitutions to give $LiMn_{2-y}M_yO_4$ (M = Li, Cr, Fe, Co, Ni, and Cu) [15,16]. The $LiMn_{2-2y}Li_yNi_yO_4$ samples were found to exhibit excellent cyclability both at ambient and elevated temperatures, rate capability, and storage characteristics. The remarkable improvement in performance was attributed to a suppression of the lattice parameter difference between the two cubic phases formed during the charge–discharge process and the consequent lowering of microstrain. However, the reversible capacity values of $LiMn_{2-2y}Li_yNi_yO_4$ were reduced to around 100 mA h/g compared to the 120 mA h/g achieved with the conventional $LiMn_2O_4$. With an aim to enhance further the understanding of the factors that influence the electrochemical performance, we focus here

* Corresponding author. Tel.: +1-512-471-1791; fax: +1-512-471-7681.
E-mail address: rmanth@mail.utexas.edu (A. Manthiram).

0378-7753/$ – see front matter © 2003 Elsevier B.V. All rights reserved.
doi:10.1016/j.jpowsour.2003.09.059

on a comparison of the electrochemical properties of two sets of $LiMn_{2-y-z}Li_yNi_zO_4$ samples: one set of samples were obtained by standard solid state reactions as in our previous investigations [15,16] and the other set of samples were obtained by reacting a $Li_{\sim 0.5}MnO_2$ precursor supplied by a commercial firm with appropriate amounts of lithium hydroxide and nickel hydroxide. The latter $LiMn_{2-y-z}Li_yNi_zO_4$ samples are found to exhibit even better capacity retention than the former and the differences in the electrochemical performances between the two sets of samples are correlated to the differences in particle size and distribution.

2. Experimental

The $LiMn_{2-y-z}Li_yNi_zO_4$ samples were synthesized by two different procedures. Procedure 1 involved a solid state reaction of required amounts of Li_2CO_3, Mn_2O_3, and NiO at 800 °C for 48 h in air to give $LiMn_{2-y-z}Li_yNi_zO_4$ ($0 \leq y \leq 0.075$ and $0 \leq z \leq 0.075$) [15,16], which is designated hereafter as oxide method. Procedure 2 involved the use of a $Li_{\sim 0.5}MnO_2$ precursor supplied by Carus Chemical Company. Atomic absorption spectroscopic (AAS) analysis of the $Li_{\sim 0.5}MnO_2$ precursor indicated a Li:Mn ratio of 0.515:0.985 and therefore on firing at 800 °C for 48 h in air, the precursor yielded the spinel oxide $LiMn_{1.97}Li_{0.03}O_4$. The $LiMn_{2-y-z}Li_yNi_zO_4$ ($0.03 \leq y \leq 0.05$ and $0 \leq z \leq 0.06$) compositions were obtained by mixing the $Li_{0.515}Mn_{0.985}O_2$ precursor with required amounts of $LiOH{\cdot}H_2O$ and $Ni(OH)_2{\cdot}xH_2O$ followed by firing at 800 °C for 48 h in air, which is hereafter designated as precursor method. The $Ni(OH)_2{\cdot}xH_2O$ sample was obtained by adding lithium hydroxide into $Ni(CH_3COO)_2$ solution followed by filtering and washing the precipitate. The Ni content in the $Ni(OH)_2{\cdot}xH_2O$ precipitate thus obtained was determined by atomic absorption spectroscopy (AAS).

All the $LiMn_{2-y-z}Li_yNi_zO_4$ samples were characterized by X-ray powder diffraction. Particle size and morphology of the samples were studied with a JEOL JSM-5610 scanning electron microscope (SEM). Brunauer–Emmett–Teller (BET) surface areas were measured with a Quantachrome Autosorb-1 analyzer. Electrochemical performances of the cathodes were evaluated with CR2032 coin cells fabricated with metallic lithium anode and 1 M $LiPF_6$ in ethylene carbonate (EC) and diethyl carbonate (DEC) electrolyte (EM Industries Inc.) between 4.3 and 3.5 V at both room temperature and 60 °C at various rates ranging from C/10 to 4C. The cathodes were fabricated by mixing 75 wt.% $LiMn_{2-y-z}Li_yNi_zO_4$ powder, 20 wt.% acetylene black, and 5 wt.% polytetrafluoroethylene (PTFE) binder. Manganese dissolution was measured by storing the sample powder in 1 M $LiPF_6$ in EC/DEC electrolyte at 55 °C for 7 days and analyzing the Mn content by atomic absorption spectroscopy.

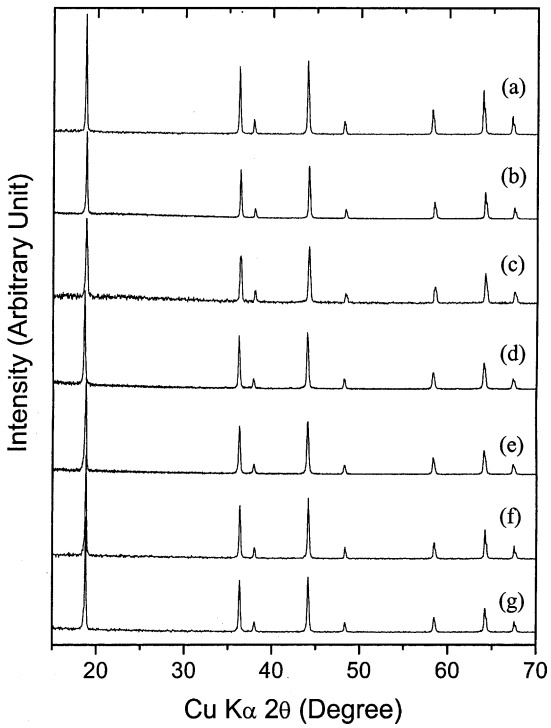

Fig. 1. X-ray diffraction patterns of (a) $LiMn_2O_4$, (b) $LiMn_{1.9}Li_{0.05}Ni_{0.05}O_4$, (c) $LiMn_{1.88}Li_{0.06}Ni_{0.06}O_4$, (d) $LiMn_{1.85}Li_{0.075}Ni_{0.075}O_4$, (e) $LiMn_{1.97}Li_{0.03}O_4$, (f) $LiMn_{1.91}Li_{0.04}Ni_{0.05}O_4$, and (g) $LiMn_{1.89}Li_{0.05}Ni_{0.06}O_4$. The samples (a)–(d) were obtained by the oxide method and samples (e)–(g) were obtained by the precursor method (see Section 2 for details).

3. Results and discussion

Fig. 1 shows the X-ray diffraction patterns of the $LiMn_{2-y-z}Li_yNi_zO_4$ samples obtained by both the methods. They all have the cubic spinel structure without any impurity phases. The lattice parameter, surface area, and dissolved manganese values are given in Table 1. With a given synthesis method, the lattice parameter decreases with increasing Li and Ni content due to an increase in the oxidation state of Mn. The surface area values are in the range of $4 \pm 2\,m^2/g$ and they do not vary significantly between the two synthesis methods. However, the amount of dissolved manganese differs between the two methods and the samples prepared by the precursor method (procedure 2) appear to experience a slightly higher amount of manganese dissolution (see later).

Table 1 also gives the capacity values, and the observed capacity values are close to the theoretical values for the cation substituted samples. Fig. 2 compares the cyclability of the samples obtained by the two methods at both room temperature and 60 °C at C/5 rate, and Table 1 gives the percentage capacity loss in 50 cycles. The $LiMn_{1.97}Li_{0.03}O_4$ sample obtained by the precursor method (procedure 2) exhibits much better cyclability than the stoichiometric $LiMn_2O_4$ sample obtained by the oxide method (procedure 1), which could be due to the partial substitution of Mn by Li. For instance,

Table 1
Summary of sample characteristics

Sample no.	Synthesis method[a]	Composition	Lattice parameter (Å)	BET surface area (m^2/g)	Mn dissolution (%)	Theoretical capacity (mA h/g)[b]	Initial capacity (mA h/g)	Percentage capacity loss in 50 cycles	
								25 °C	60 °C
1	Oxide method	$LiMn_2O_4$	8.2489	3.0	1.8	148	119	39.4	53.0
2	Oxide method	$LiMn_{1.95}Li_{0.05}O_4$	8.2319	3.4	1.8	128	122	9.6	21.1
3	Oxide method	$LiMn_{1.9}Li_{0.05}Ni_{0.05}O_4$	8.2181	4.6	1.4	114	114	3.2	7.4
4	Oxide method	$LiMn_{1.88}Li_{0.06}Ni_{0.06}O_4$	8.2138	2.3	1.9	105	105	2.0	6.4
5	Oxide method	$LiMn_{1.85}Li_{0.075}Ni_{0.075}O_4$	8.2080	2.9	1.7	94	95	0.9	2.6
6	Precursor method	$LiMn_{1.97}Li_{0.03}O_4$	8.2222	5.9	4.6	136	129	8.1	24.5
7	Precursor method	$LiMn_{1.91}Li_{0.04}Ni_{0.05}O_4$	8.2103	3.0	4.6	117	111	1.0	5.4
8	Precursor method	$LiMn_{1.89}Li_{0.05}Ni_{0.06}O_4$	8.2059	4.6	2.3	109	102	0.1	2.2

[a] Oxide method involved a firing of Li_2CO_3, Mn_2O_3, and NiO, while the precursor method involved a firing of the precursor $Li_{0.515}Mn_{0.985}O_2$ with $LiOH{\cdot}H_2O$ and $Ni(OH)_2{\cdot}xH_2O$ (see Section 2).

[b] The theoretical capacity values were calculated assuming Ni^{2+} in the initial sample and based on the oxidation of only Mn^{3+} to Mn^{4+} below the cutoff charge voltage of 4.3 V.

a $LiMn_{1.95}Li_{0.05}O_4$ sample obtained by the oxide method also exhibited much better capacity retention than $LiMn_2O_4$ [15,16]. It should be noted that most of the commercially available spinel oxide samples are lithium-rich, and therefore, their cycling performance would be similar to that of the $LiMn_{1.97}Li_{0.03}O_4$ sample in Fig. 2. More importantly, the co-substituted $LiMn_{2-y-z}Li_yNi_zO_4$ samples exhibit superior capacity retention, irrespective of the synthesis method, both at room temperature and at 60 °C compared to both

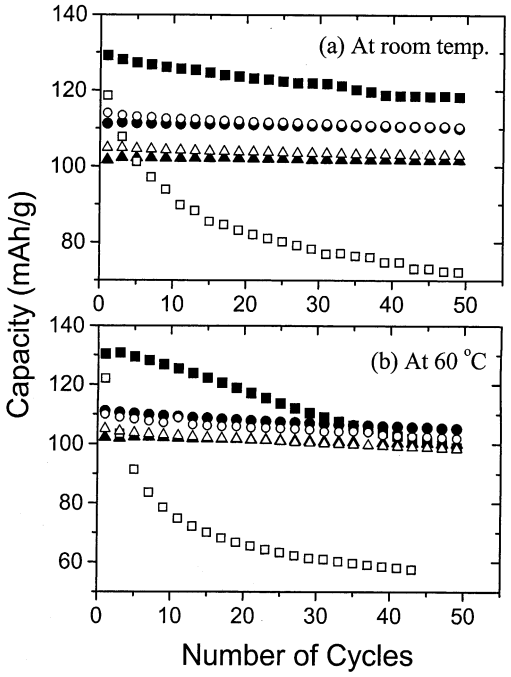

Fig. 2. Electrochemical cycling performances at (a) room temperature and (b) 60 °C at C/5 rate of the $LiMn_{2-y-z}Li_yNi_zO_4$ samples. Open symbols and solid symbols refer, respectively, to samples obtained by the oxide and precursor methods: (□) $LiMn_2O_4$, (■) $LiMn_{1.97}Li_{0.03}O_4$, (○) $LiMn_{1.9}Li_{0.05}Ni_{0.05}O_4$, (●) $LiMn_{1.91}Li_{0.04}Ni_{0.05}O_4$, (△) $LiMn_{1.88}Li_{0.06}Ni_{0.06}O_4$, and (▲) $LiMn_{1.89}Li_{0.05}Ni_{0.06}O_4$.

$LiMn_2O_4$ and $LiMn_{1.97}Li_{0.03}O_4$ (Fig. 2 and Table 1). For a given amount of Li and Ni co-substitutions (*y* and *z* values), the samples obtained by the precursor method, however, show slightly better capacity retention than those obtained by the oxide method. For example, $LiMn_{1.89}Li_{0.05}Ni_{0.06}O_4$ obtained by the precursor method loses only 2.2% of the capacity in 50 cycles at 60 °C compared to 6.4% loss for $LiMn_{1.88}Li_{0.06}Ni_{0.06}O_4$ obtained by the oxide method. Interestingly, the capacity values do not differ much between the two synthesis methods.

Fig. 3 compares the discharge profiles recorded at different C-rates for the samples obtained by both the methods. For a comparison, the data for $LiCoO_2$ cathodes are also shown in Fig. 3. The data were obtained by first charging the cathodes at C/5 rate and then discharging at various rates (C/10 to 4C rates) between 4.3 and 3.5 V. The co-substituted $LiMn_{2-y-z}Li_yNi_zO_4$ samples exhibit remarkable rate capability compared to both the $LiMn_2O_4$ cathode obtained by the oxide method and the $LiMn_{1.97}Li_{0.03}O_4$ cathode obtained by the precursor method. For a given amount of Li and Ni co-substitutions (*y* and *z* values), the rate capability does not vary significantly between the two synthesis methods. More importantly, the $LiMn_{2-y-z}Li_yNi_zO_4$ samples exhibit better rate capability than the presently used $LiCoO_2$ cathodes. For example, $LiMn_{1.89}Li_{0.05}Ni_{0.06}O_4$ retains 93.2% of its C/10 rate capacity on going to 4C rate, while $LiCoO_2$ retains 91% under similar conditions. The excellent rate capability of the $LiMn_{2-y-z}Li_yNi_zO_4$ cathodes makes them attractive particularly for electric vehicles.

Fig. 4 compares the storage characteristics of the samples obtained by both the synthesis methods. The storage performance data were evaluated by subjecting the coin cells at C/5 rate to one charge–discharge cycle at room temperature between 4.3 and 3.5 V followed by discharging to various depths of discharge (DOD) in the second cycle, storing at 60 °C for 7 days at various DOD, completing the second discharge cycle after cooling to room temperature, and evaluating the full discharge capacity in the third cycle

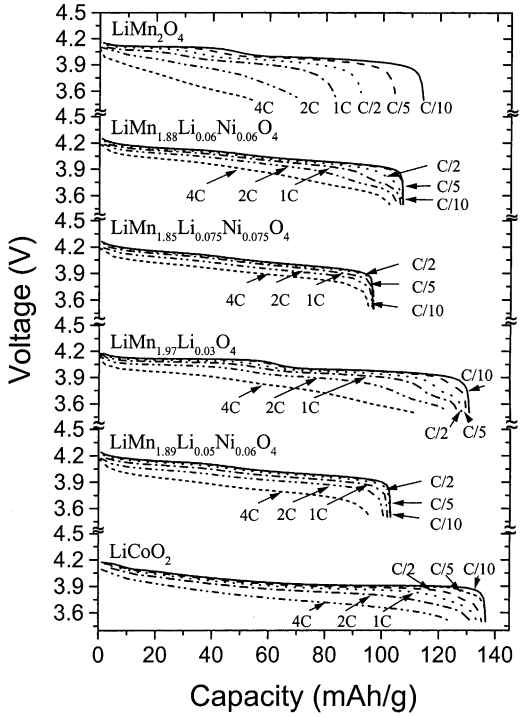

Fig. 3. Comparison of the discharge profiles illustrating the rate capabilities of the $LiMn_{2-y-z}Li_yNi_zO_4$ samples obtained by the two synthesis methods and $LiCoO_2$. $LiMn_2O_4$, $LiMn_{1.88}Li_{0.06}Ni_{0.06}O_4$, and $LiMn_{1.85}Li_{0.075}Ni_{0.075}O_4$ were obtained by the oxide method while $LiMn_{1.97}Li_{0.03}O_4$ and $LiMn_{1.89}Li_{0.05}Ni_{0.06}O_4$ were obtained by the precursor method.

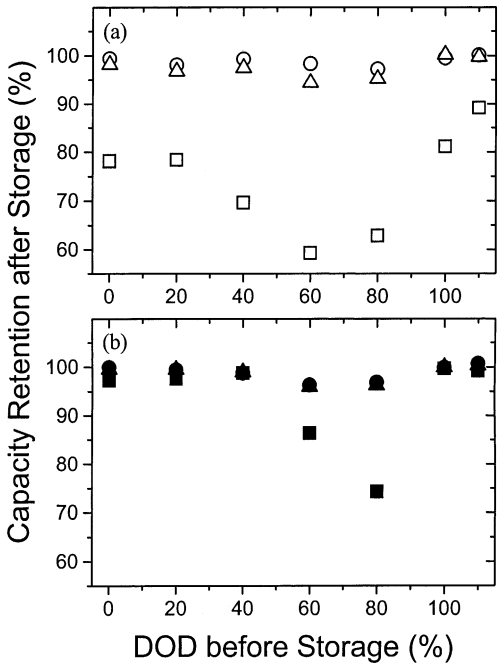

Fig. 4. Comparison of the percentage capacity retention after storing at 60 °C for 7 days at different DOD. Open symbols and solid symbols refer, respectively, to samples obtained by the oxide and precursor methods: (□) $LiMn_2O_4$, (■) $LiMn_{1.97}Li_{0.03}O_4$, (●) $LiMn_{1.91}Li_{0.04}Ni_{0.05}O_4$, (▲) $LiMn_{1.89}Li_{0.05}Ni_{0.06}O_4$, (○) $LiMn_{1.85}Li_{0.075}Ni_{0.075}O_4$, and (△) $LiMn_{1.8}Li_{0.1}Ni_{0.1}O_4$.

at room temperature. The percentage capacity retention in Fig. 4 after storing at various DOD was obtained as a ratio of the third discharge capacity to the first discharge capacity. While both $LiMn_2O_4$ obtained by the oxide method and $LiMn_{1.97}Li_{0.03}O_4$ obtained by the precursor method lose significant amount of capacity after storage (up to 25–40% at 60–80% DOD) similar to that found by others [17], the co-substituted $LiMn_{2-y-z}Li_yNi_zO_4$ cathodes retain >95% of their initial capacity, demonstrating excellent storage characteristics. The storage characteristics do not vary significantly between the two synthesis methods.

The electrochemical performance data in Figs. 2–4 reveal that for a given amount of Li and Ni co-substitutions (y and z values) in $LiMn_{2-y-z}Li_yNi_zO_4$, the synthesis method does not influence the rate capability and storage properties (Figs. 3 and 4), but does affect the cyclability (Fig. 2). With an aim to understand the origin of the differences in cyclability, we have compared the SEM data of some samples that have nearly the same composition (y and z values), but differ in the synthesis methods. Fig. 5 compares the SEM photographs of $LiMn_{1.88}Li_{0.06}Ni_{0.06}O_4$ obtained by the oxide method and $LiMn_{1.89}Li_{0.05}Ni_{0.06}O_4$ obtained by the precursor method, both having nearly the same composition. While the sample obtained by the oxide method has a non-uniform distribution of particle size (1–10 μm) (Fig. 5a), the sample obtained by the precursor method has a more uniform distribution of particle size (∼10 μm) without any particles of <5 μm (Fig. 5b). Also, the primary particles of the samples obtained by the oxide method are larger with >2 μm (Fig. 5c), while those of the sample obtained by the precursor method are smaller with ∼0.5 μm and are more uniform (Fig. 5d). Similar differences in microstructures depending on the synthesis method were found for other compositions as well.

With a given amount of Li and Ni co-substitutions in $LiMn_{2-y-z}Li_yNi_zO_4$, the better cyclability of the samples obtained by the precursor method (Fig. 2) could be due to the larger and more uniform size of the secondary particles (Fig. 5b) compared to that of the sample obtained by the oxide method (Fig. 5a). On the other hand, the higher amount of manganese dissolution encountered with the samples obtained by the precursor method (Table 1) could be due to the smaller size of the primary particles (Fig. 5d) compared to that of the samples obtained by the oxide method (Fig. 5c). The better cyclability of the samples obtained by the precursor method despite a higher manganese dissolution suggests that manganese dissolution may not be the primary or most important reason for the capacity fade of the spinel manganese oxides. This conclusion is further reinforced by the fact that the co-substituted samples exhibit superior capacity retention compared to $LiMn_2O_4$ (samples 1–5 in Table 1) although the manganese dissolution remains nearly the same. We believe the microstrain developing from a larger lattice parameter difference between the two cubic phases formed during the charge–discharge cycling may be the primary capacity fading mechanism of the spinel manganese oxides.

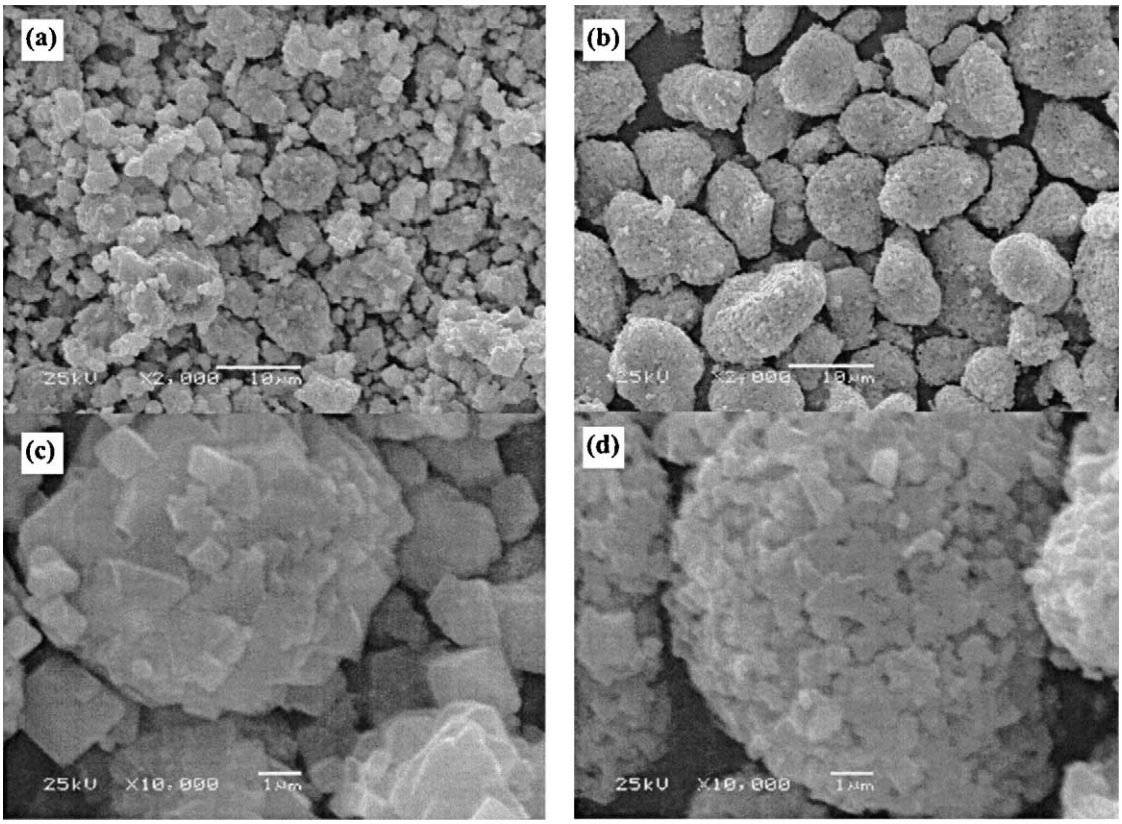

Fig. 5. SEM photographs of $LiMn_{1.88}Li_{0.06}Ni_{0.06}O_4$ obtained by the oxide method and $LiMn_{1.89}Li_{0.05}Ni_{0.06}O_4$ obtained by the precursor method: (a) $LiMn_{1.88}Li_{0.06}Ni_{0.06}O_4$ at low magnification, (b) $LiMn_{1.89}Li_{0.05}Ni_{0.06}O_4$ at low magnification, (c) $LiMn_{1.88}Li_{0.06}Ni_{0.06}O_4$ at high magnification, and (d) $LiMn_{1.89}Li_{0.05}Ni_{0.06}O_4$ at high magnification.

4. Conclusions

A co-substitution of small amounts of Li and Ni to give $LiMn_{2-y-z}Li_yNi_zO_4$ ($0.04 \leq y \leq 0.075$ and $0.05 \leq z \leq 0.075$) is found to lead to superior capacity retention, rate capability, and storage characteristics compared to both the stoichiometric $LiMn_2O_4$ and lithium-rich $LiMn_{1.97}Li_{0.03}O_4$ spinel oxides. With the co-substituted $LiMn_{2-y-z}Li_yNi_zO_4$ samples, the microstructure is found to influence the cyclability, but not the rate capability or storage characteristics. Samples with larger and more uniform secondary particles, but with smaller primary particles, are found to give better cyclability despite a higher amount of manganese dissolution arising from smaller primary particles. The study suggests that factors other than manganese dissolution may play a dominant role in the capacity fading mechanism of spinel manganese oxides. In fact, the superior cyclability of the co-substituted $LiMn_{2-y-z}Li_yNi_zO_4$ samples have been attributed to the smaller lattice parameter difference between the two cubic phases formed during charge–discharge cycles and the consequent suppression of lattice strain [15,16]. The superior cyclability, high rate capability, and excellent storage characteristics of $LiMn_{2-y-z}Li_yNi_zO_4$ coupled with the low cost and environmentally benign nature of Mn may make these cathodes attractive for electric vehicle applications.

Acknowledgements

This work was supported by the NASA Glenn Research Center and the Welch Foundation Grant F-1254.

References

[1] M.M. Thackeray, Y. Shao-Horn, A.J. Kahaian, K.D. Kepler, E. Skinner, J.T. Vaughey, S.A. Hackney, Electrochem. Solid-State Lett. 1 (1998) 7.
[2] D.H. Jang, Y.J. Shin, S.M. Oh, J. Electrochem. Soc. 143 (1996) 2204.
[3] T. Inoue, M. Sano, J. Electrochem. Soc. 145 (1998) 3704.
[4] H. Huang, C.A. Vincent, P.G. Bruce, J. Electrochem. Soc. 146 (1999) 3649.
[5] S.-C. Park, Y.-S. Han, Y.-S. Kang, P.S. Lee, S. Ahn, H.-M. Lee, J.-Y. Lee, J. Electrochem. Soc. 148 (2001) A680.
[6] D. Aurbach, M.D. Levi, K. Gamulski, B. Markovsky, G. Salitra, E. Levi, U. Heider, L. Heider, R. Oesten, J. Power Sources 81 (1999) 472.
[7] J.H. Lee, J.K. Hong, D.H. Jang, Y.-K. Sun, S.M. Oh, J. Power Sources 89 (2000) 7.
[8] Y. Xia, M. Yoshio, J. Power Sources 66 (1997) 129.

[9] Y. Shin, A. Manthiram, Electrochem. Solid-State Lett. 5 (2002) A55.
[10] A.M. Kannan, A. Manthiram, Electrochem. Solid State Lett. 5 (2002) A167.
[11] Y.-S. Lee, N. Kumada, M. Yoshio, J. Power Sources 96 (2001) 376.
[12] Y.-S. Hong, C.-H. Han, K. Kim, C.-W. Kwon, G. Campet, J.-H. Choy, Solid State Ionics 139 (2001) 75.
[13] R.J. Gummow, A. De Kock, M.M. Thackeray, Solid State Ionics 69 (1997) 59.
[14] A.D. Robertson, S.H. Lu, W.F. Howard Jr., J. Electrochem. Soc. 144 (1997) 3505.
[15] Y. Shin, A. Manthiram, Electrochem. Solid State Lett. 6 (2003) A34.
[16] Y. Shin, A. Manthiram, Chem. Mater. 15 (2003) 2954.
[17] T. Saito, M. Machida, Y. Yamamoto, M. Nagamine, in: Proceedings of the 200th Meeting of the Electrochemical Society, Abstract No. 180, San Francisco, September 2–7, 2001.